(Title page)

STUDY ON THE HYDRODYNAMICS OF THE EBRO RIVER LOWER COURSE USING TRITIUM AS A RADIOTRACER

Dr. Joan Albert Sanchez-Cabeza (To whom correspondence should be addressed)
Departament de Física, Facultat de Ciències, Edifici Cc
Universitat Autònoma de Barcelona, 08193 BELLATERRA, Barcelona (Spain)
Tel: +343-581.19.15
FAX: +343-581.21.55
E-mail: JA.SANCHEZ@CC.UAB.ES

Dr. Lluís Pujol
Departament de Física, Facultat de Ciències, Edifici Cc
Universitat Autònoma de Barcelona, 08193 BELLATERRA, Barcelona (Spain)
Tel.:. +343-581.11.91
FAX: +343-581.21.55
E-mail: IFFR3@CC.UAB.ES

Short Title: Ebro river hydrodynamics using tritium...

Abstract

Tritium routinely released as low-activity liquid radioactive waste by the Ascó nuclear power plant (Tarragona, Spain) was used as a radiotracer to study the hydrodynamics of the Ebro river (northeastern Spain) lower course. In co-ordination with the plant, a field experiment was carried out in which, after a tritium release, water was sampled downstream from nine locations along the river at periodic intervals. Tritium was measured with a low-background liquid scintillation system and the concentration time evolution for each location was obtained. In order to study the river hydrodynamics, the one-dimensional advection-diffusion equation was used to determine the longitudinal dispersion coefficient and mean velocity of Ebro river waters. Experimental data were fitted using an analytical, a box–type and a numerical model to solve the equation. For the studied river discharge, namely 220 m^3 s^{-1}, the longitudinal dispersion coefficient ranged from 67 ± 20 to 294 ± 36 m^2 s^{-1} and the mean water velocity ranged from 0.575 ± 0.002 m s^{-1} to 0.710 ± 0.014 m s^{-1} depending on the sampling point. From the analysis of the longitudinal dispersion coefficient it was observed that this river section shows three zones with different hydrodynamics which largely depends on the river morphology.

Key words: River hydrodynamics, Longitudinal dispersion coefficient, Tritium, Mathematical model, Uncertainty, Environmental radioactivity

STUDY ON THE HYDRODYNAMICS OF THE EBRO RIVER LOWER COURSE USING TRITIUM AS A RADIOTRACER

J.A. Sanchez-Cabeza and Ll. Pujol

Departament de Física, Universitat Autònoma de Barcelona, 08193 Bellaterra, Spain

Abstract

Tritium routinely released as low-activity liquid radioactive waste by the Ascó nuclear power plant (Tarragona, Spain) was used as a radiotracer to study the hydrodynamics of the Ebro river (northeastern Spain) lower course. In co-ordination with the plant, a field experiment was carried out in which, after a tritium release, water was sampled downstream from nine locations along the river at periodic intervals. Tritium was measured with a low-background liquid scintillation system and the concentration time evolution for each location was obtained. In order to study the river hydrodynamics, the one-dimensional advection-diffusion equation was used to determine the longitudinal dispersion coefficient and mean velocity of Ebro river waters. Experimental data were fitted using an analytical, a box–type and a numerical model to solve the equation. For the studied river discharge, namely 220 m^3 s^{-1}, the longitudinal dispersion coefficient ranged from 67 ± 20 to 294 ± 36 m^2 s^{-1} and the mean water velocity ranged from 0.575 ± 0.002 m s^{-1} to 0.710 ± 0.014 m s^{-1} depending on the sampling point. From the analysis of the longitudinal dispersion coefficient it was observed that this river section shows three zones with different hydrodynamics which largely depends on the river morphology.

Keywords: River hydrodynamics, Longitudinal dispersion coefficient, Tritium, Mathematical model, Uncertainty, Environmental radioactivity.

NOMENCLATURE

$A(x,t)$	mathematical function.
$c(x,t)$	mean cross sectional concentration of the pollutant or tracer.
$c_{x,t+\Delta t}$	mean cross sectional concentration, as a function of time, for a distance x from the release point (explicit numerical model).
c_i^{exp}	experimental tritium concentration.
c_i^{the}	theoretical tritium concentration (for each model).
C_i	background tracer concentration.
C_0	initial mean cross sectional concentration after total mixing.
C_t	mean concentration of tracer release.
d	mean depth.
D	longitudinal dispersion coefficient.
D_o	optimized longitudinal dispersion coefficient.
erfc(x)	complementary error function.
F_i	experimental data for chi–square fitting.
k_b	dispersion coefficient in the box–type model.
k'_b	numerical dispersion coefficient in the box–type model.
$k_{i,1}$	transfer coefficient from compartment i to compartment i+1.
$k_{i,2}$	transfer coefficient from compartment i to compartment i-1.
L	mixing length.
m	number of experimental observations.
n	Manning roughness coefficient.
N_i	tracer particles in box i.
q	tracer release flow rate.
Q	river discharge.
$Q_i(t)$	tracer sources.
R	hydraulic radius.
s^2	variance.
S	slope.
S_i	compartment i surface.
t	time.
Δt	temporal resolution of the box–type and numerical models.
U	mean flow velocity.

U_o	optimised velocity.
V_i	compartment *i* volume.
w	channel width.
w_{ij}	matrix W elements.
W	function derivative respect the estimated parameters (matrix).
W'	transpose of the matrix W.
$(W'W)^{-1}$	covariance matrix.
x	distance in the flow direction.
x_i	independent variable.
Δx	spatial resolution of the box–type and numerical models.
y_i	dependent variable.
$\hat{y}_i$	estimate value of the dependent variable.
α	model estimated parameter.
β	model estimated parameter.
ε	statistical significance risk level.
χ^2	chi-square.
χ^2_ε	statistically significant χ^2 with risk level ε.
λ	decay constant.
ϕ_i	theoretical data for chi–square fitting.
θ_j	general parameter estimated in a model.
σ_α	α parameter uncertainty.
σ_β	β parameter uncertainty.

INTRODUCTION

Numerous experimental studies in the hydrosphere have been carried out to determine the velocity and longitudinal dispersion coefficient in rivers using tracers through the one-dimensional advection-diffusion equation expressed as:

$$\frac{\partial c(x,t)}{\partial t} = D\frac{\partial^2 c(x,t)}{\partial x^2} - U\frac{\partial c(x,t)}{\partial x} \quad (1)$$

where $c(x,t)$ is the tracer concentration, D is the longitudinal dispersion coefficient and U is the mean flow velocity. In most of these studies, chemical or fluorescent tracers are used, although they have various drawbacks, as they are usually non-perfectly conservative, their degradation products can be toxic, and they are relatively expensive (Graf, 1995; Clark *et al.*, 1996). On the other hand, natural and artificial radionuclides have been extensively used as tracers in the marine, fluvial and groundwater environments in order to estimate water body movements (Bertin and Bourg, 1994; Sanchez-Cabeza *et al.*, 1995; Hancock and Murray, 1996). In particular, the use of tritium as a tracer in river waters has several advantages (Guizerix and Florkowski, 1983):

1. It is an ideal tracer as it forms water (HTO) molecules.
2. It does not adsorb to sediments.
3. Sampling is easy and it does not require special techniques.
4. Small sample amounts can be used and extremely low tritium concentrations in water can be measured by low-background liquid scintillation.
5. The relatively long half-life of tritium permits storage before measurement.

In this study, tritium routinely released as low-activity liquid radioactive waste by the Ascó nuclear power plant (Tarragona, Spain), was used as a radiotracer to determine the longitudinal dispersion coefficient and mean velocity of the Ebro river waters

(northeastern Spain). The analysis of both parameters can be used to qualitatively understand the main morphological characteristics of the Ebro river in its lower course.

The mixing process of a continuous release can be divided into three zones (Yotsukura and Sayre, 1976; IAEA, 1985; Scott, 1994):

1. Initial mixing zone: the effluent (or tracer) is discharged into the river with an initial momentum and is not fully mixed. This zone extends from the source to a section where the distribution of tracer concentration becomes uniform over depth, but not horizontally, and may cover a distance of up to about one hundred times the depth of the river channel. In this first stage three-dimensional equations are needed to study the dispersion.
2. Full mixing zone: the effluent has lost its initial momentum. This stage extends from the end of the initial mixing zone to a section where the tracer is mixed over the full cross-section of the water body, that is vertically and horizontally, and may cover from 3 to 10 km in large rivers. The distance from the source to the point in which mixing is homogeneous and complete is known as the mixing length. To model this stage two-dimensional equations are needed.
3. Far field dispersion zone: this stage extends from the end of the full mixing zone to a long distance, where the tracer concentration may become undetectable. One-dimensional equations are used to model this zone. Apart from convective transport, the predominant effect in this stage is longitudinal dispersion, that is, tracer cloud stretching in the velocity direction. This is predominant for instantaneous and non-continuous releases.

One of the important assumptions of the tracer dilution principle in the third zone is full mixing. In this case, and also for a continuous release under stationary hydraulic conditions, the tracer activity in the river (C_o) can be calculated as

$$C_o = \frac{C_t}{Q} \cdot q \tag{2}$$

where C_t is the mean concentration of tracer release, q is the flow rate of the tracer discharge and Q is the river discharge. This is valid for sampling points located at a distance from the source greater than the mixing length. A number of empirical formulae have been proposed to estimate the mixing length (L):

1. Day (1977):

$$L = 25w \tag{3}$$

where w is the channel width.

2. Hull (Guizerix and Florkowski, 1983): this empirical formula is based on experience in gauging numerous rivers but in general underestimates the mixing length:

$$L = \sqrt{\frac{w^3}{d}} \tag{4}$$

where w and d are the stream mean width and depth, respectively.

Nevertheless, these expressions should be used with caution as they have been empirically established for particular rivers in specific hydraulic conditions. In the case of the Ebro river, Asociación Nuclear Ascó (personal communication) observed that full heat mixing was always observed at 6.5 km from the release point for a range of hydraulic conditions. As a consequence, in this work, we studied far-field tracer dispersion through Eq. (1) after this point, and was justified by the results of the experiment.

STUDY AREA

The Ebro river is the largest Spanish fluvial system discharging into the western Mediterranean sea. It is located in northeastern Spain and it flows through several large cities and agricultural, mining and industrial areas. The river is 928 km long, has a 85,550 km^2 drainage basin and ends at the Ebro Delta, a 320 km^2 sedimentary zone which is one of the most important wetlands in the western Mediterranean area (Palanques *et al.*, 1990; Forés *et al.,* 1992; Ibáñez *et al.,* 1996). The Ebro river basin covers several geological terrains: the sedimentary and metamorphic Palaeozoic terrains of the Iberian and Pyrenees mountains, the igneous terrains of these two areas and of the Priorat Massif, the sedimentary Mesozoic terrains of the Iberian Chain and the sedimentary Tertiary terrains of the Pre-Pyrenees and the Ebro Valley. The lower part of the Ebro river flows across the Neogene Mora Depression, bends through the Catalan Chain and the Baix Ebre Valley, and flows across the delta plain deposits (Guillén and Palanques, 1992) (Fig. 1).

The Ebro river monthly water discharge is quite irregular. The northern tributaries provide a greater contribution to the discharge than those in the south because the former drainage basins are located in higher rainfall areas. There has been a significant decrease in the mean river discharge during this century: the mean discharge in the first third of the century (1914-1935) was 592 $m^3\ s^{-1}$, whereas in the last few decades (1960-1990) it was 426 $m^3\ s^{-1}$, that is, a 28 % reduction (Ibáñez *et al.,* 1996). This can be explained by rainfall decrease in the Ebro basin and by the increase in water use for human activities (reservoirs, human consumption, agriculture, industry), causing stronger evaporation and underground filtration. In fact, at Xerta some water is diverted for agricultural and human consumption purposes.

The Ascó nuclear power plant is established in the final section of the river and comprises two Pressurised water reactor (PWR) units: Ascó I and Ascó II (Fig. 2). During their normal operation, these two units generate low-activity radioactive liquid waste, including tritium, which is released into the river in a controlled way: most activity is released from storage tanks, although a continuous release also exists. This routine operation was used to trace river waters downstream.

METHODS

Sampling

In order to study the hydrological dispersion of conservative pollutants in the Ebro river waters, one tank release was followed at nine different locations during 19–20 May 1992, in co-ordination with the Ascó nuclear power plant (Fig. 2). During the field experiment, the flow rate was kept constant at 220 $m^3 s^{-1}$ by the Ribaroja and Flix dams, upstream from Ascó. Somewhat lower values were observed downstream, as some water is diverted at Xerta for agricultural and human consumption purposes after the corresponding sampling point. The release characteristics are shown in Table 1. Sampling locations were selected on the basis of the following criteria:

1. Higher spatial resolution near the source (four sampling points in 16 km), and a sampling point approximately every ten kilometres until the town of Amposta.
2. Easy access to sampling locations. The towns with river pier were preferred.

Before the field experiment, the tracer transit time and dispersion was estimated using an empirical gaussian model based on data collected during previous field experiments (Sanchez-Cabeza *et al.,* 1992) in which the velocity and dispersion coefficient are assumed to be constant.

In the chosen locations, water was sampled every 15 minutes during a total sampling period which ranged from 4 to 15 hours, depending on the distance from the nuclear power plant and the river flow (Table 2). Special attention was given to the collection and preservation of samples (Keith *et al.,* 1983; APHA, 1992): a total of 332 water samples of 125 ml were collected in polyethylene bottles, which had been carefully washed in the laboratory. Water was collected, as far as possible, at a certain distance from the riverbed and sufficiently far from the border, natural or artificial obstacles, and avoiding stagnant or turbid water zones. Before the sample was collected, containers were rinsed three times with flowing river water. Finally, samples were taken to the laboratory for analysis.

Analysis

As tritium is a soft beta emitter (5.72 keV mean energy), liquid scintillation is the most appropriate technique for its measurement. In this work, the low-background liquid scintillation spectrometer Quantulus 1220 (Wallac) was used to determine tritium in river water samples (Sanchez-Cabeza *et al.,* 1993; Pujol, 1996).

The analytical method used to determine tritium in river water samples was, briefly, the following: (*i*) samples were filtered through slow depth filters (such as Whatman 542), (*ii*) 8 ml of the filtrate was mixed and vigorously shaken during one minute with 12 ml of the scintillation cocktail OptiPhase Hisafe 3 (Wallac) in polyethylene vials (Wallac), (*iii*) three background samples and three tritium standards were simultaneously prepared, (*iv*) samples, backgrounds and tritium standards were stored in the system during at least one day so that chemiluminescence, which interferes with tritium measurements, had sufficiently decreased, and (*v*) samples, backgrounds and tritium standards were counted using Quantulus 1220 (Wallac) during 360 minutes.

RESULTS

Field study

The time evolution of tritium concentration in Ebro river waters at all locations is shown in Fig. 3. A peak distribution was clearly observed for all locations, showing variable maxima, both in concentration and time. In general, the tritium concentration maximum decreased downstream the release point. It must be stressed that the observed concentrations do not represent any radiological risk to the population (Pujol and Sanchez-Cabeza, 1997).

The tritium peak maximum and total area (equal to the measured activity) observed at Ascó was lower than that observed at other locations, indicating that full mixing was not yet attained, in agreement with the mixing length estimated above. On the other hand, the total activity observed at Pas de l'Ase (79±3 GBq) was totally consistent with the released activity, 76.5 GBq (Moya, personal communication). The shape of the tritium concentration peak in Pas de l'Ase and García is different from that observed at other locations. Furthermore, the tritium concentration maximum quickly decreases between García and Mora de Ebro, indicating the importance of longitudinal diffusion in this zone. Contrarily, the shape of the tritium pulses from Mora de Ebro to Tortosa is similar, thus manifesting a lower importance of this phenomenon.

The tritium concentration peaks at Xerta and Tortosa were incomplete. This indicated that the water velocity in this area had been overestimated and stressed the need, in further field experiments, to take into account the effect of slope changes in velocity and dispersion estimations. Also, it should be born in mind that part of the river flow is diverted at Xerta for agricultural and human consumption purposes, thus slightly varying the total river flow rate. Furthermore, the tritium pulse observed at Amposta

(Fig. 4), in the estuarine area, did not correspond to that observed at other locations, as its maximum was almost coincident with that at Tortosa. This peak was attributed to a previous release from the Ascó nuclear power plant and was concluded that transit time in this area was much slower than upstream.

Some of the tritium peaks showed a long-tail, as in Mora de Ebro and Miravet. This phenomenon is usually attributed to the irregular shape of the riverbed, which may produce water dead zones that cause tracer retention (Day, 1975; Nordin and Troutman, 1980; Yu and Wenzhi, 1989; Rutherford, 1994).

Mathematical modelling

Tracer dispersion in surface waters can be modelled using analytical, box-type and numerical solutions of the transport equations (IAEA, 1985; Scott, 1994). In this work, longitudinal dispersion coefficients and mean velocities were determined by fitting the solutions of the advection-diffusion Eq. (1) obtained for each model with the experimental data, as the far-field dispersion approximation can be assumed from Pas de l'Ase. Two exception were Ascó, where the far-field approximation was not valid, and Amposta, where estuarine effects are present.

1. Analytical model

The boundary conditions required to solve the one-dimensional advection-diffusion equation in our case are the following:

- The tritium pulsed release is described as a step function:

$$c(x,0) = C_i \tag{5}$$

$$c(0,t) = \begin{cases} C_0 & 0 < t \le t_0 \\ 0 & t > t_0 \end{cases} \tag{6}$$

- A semi-infinite flow line is assumed for the model to avoid any effect of the downstream boundary on results (Kopman and Voss, 1987):

$$\frac{\partial c}{\partial x}(\infty, t) = 0 \tag{7}$$

Then, the analytical solution to the one-dimensional advection-diffusion equation given by Van Genuchten and Alves (1982) is:

$$c(x,t) = \begin{cases} C_i + (C_0 - C_i)A(x,t) & 0 < t \le t_0 \\ C_i + (C_0 - C_i)A(x,t) - C_0 A(x, t - t_0) & t > t_0 \end{cases} \tag{8}$$

where

$$A(x,t) = \frac{1}{2}\operatorname{erfc}\left[\frac{x - Ut}{2(Dt)^{1/2}}\right] + \frac{1}{2}\mathrm{e}^{-\frac{Ux}{D}}\operatorname{erfc}\left[\frac{x + Ut}{2(Dt)^{1/2}}\right] \tag{9}$$

and erfc (x) is the complementary error function.

2. Box-type model

The time evolution of the number of atoms of a radionuclide in a compartment i is given by Abril and García León (1992):

$$\frac{\mathrm{d}}{\mathrm{d}t}N_\mathrm{i} = -k_{\mathrm{i},1}N_\mathrm{i} + k_{\mathrm{i}+1,2}N_{\mathrm{i}+1} + k_{\mathrm{i}-1,1}N_{\mathrm{i}-1} - k_{\mathrm{i},2}N_\mathrm{i} + Q_\mathrm{i}(t) - \lambda N_\mathrm{i} \tag{10}$$

where $Q_\mathrm{i}(t)$ includes all the radionuclide sources in the system and λ is the radionuclide radioactive decay constant. In our case, the radioactive decay term, λN_i, is negligible due to the rapidity of the phenomenon compared to the tritium half-life. The transfer coefficients between two adjacent compartments are given by the expressions

$$k_{\mathrm{i},1} = \frac{U_\mathrm{i}S_\mathrm{i}}{V_\mathrm{i}} + \frac{k_\mathrm{b}S_\mathrm{i}}{\Delta x_\mathrm{i}V_\mathrm{i}} \tag{11}$$

$$k_{\mathrm{i},2} = \frac{k_\mathrm{b}S_\mathrm{i}}{\Delta x_\mathrm{i}V_\mathrm{i}} \tag{12}$$

where k_b is a dispersion coefficient, V_i is the volume, S_i is the surface and Δx_i is the length, all of them referred to compartment *i*. The first term on the right hand of Eq. (11) refers to convection and the second to dispersion. In Eq. (12) only dispersion is considered, since there is no flow upstream.

The water volume exchanged by a compartment *i* during Δt must be smaller than the compartment volume V_i. Mathematically, this can be expressed as $\Delta t << 1/k_{max}$. On the other hand, the hypothesis of instantaneous and homogeneous mixing of a radionuclide input in a compartment produces numerical dispersion during calculation. This effect is equivalent to adding k_b' to the dispersion coefficient k_b according to the expression given by Prandle (1984):

$$k_b' = \frac{1}{2}(U\Delta x - U^2\Delta t) \tag{13}$$

Then, the longitudinal dispersion coefficient can be expressed as

$$D = k_b + k_b' \tag{14}$$

3. Numerical model

The solution of the one-dimensional advection-diffusion equation using an explicit finite differences method can be obtained from the expression

$$c_{x,t+\Delta t} = \left(\frac{D\Delta t}{(\Delta x)^2} - \frac{U\Delta t}{\Delta x}\right)c_{x+\Delta x,t} + \left(1 - 2\frac{D\Delta t}{(\Delta x)^2} + \frac{U\Delta t}{\Delta x}\right)c_{x,t} + \frac{D\Delta t}{(\Delta x)^2}c_{x-\Delta x,t} \tag{15}$$

where $c_{x,t}$ is the mean cross sectional concentration as a function of time for a distance *x* from the emission point. The optimization of the spatial and temporal resolution led us to choose Δx = 100 m and Δt = 15 s, respectively, for which the solution is stable (Pujol, 1996).

Parameters and uncertainties determination

Several computer codes were written to generate solutions of the advection-diffusion equation for each model and for any parameter values, longitudinal dispersion coefficient and mean velocity, at all the considered locations. For each solution and measured tritium concentration time-distribution, chi-square (χ^2) was computed using the expression

$$\chi^2 = \sum_{i=1}^{i=k} \frac{(F_i - \phi_i)^2}{\phi_i} \tag{16}$$

where F_i are the experimental data and ϕ_i are the theoretical values generated for each model. The fitted solution was obtained by minimisation of χ^2 by varying D and U, and was considered statistically acceptable if $\chi^2 \in \{\chi^2_{\varepsilon_1}, \chi^2_{\varepsilon_2}\}$ where χ^2_ε is the decision limit with ε significance level, usually chosen as $\varepsilon_1 = 0.05$ and $\varepsilon_2 = 0.95$ (Cuadras, 1991). Values above and below these limits cannot be considered in keeping with the experimental data. The D and U values for which χ^2 is minimum were called optimized longitudinal diffusion coefficient (D_o) and optimized velocity (U_o).

The parameter uncertainties were determined, briefly, as follows (Rawlings, 1988): let us consider a set of experimental data x_i (independent variable), y_i (dependent variable) and i = 1, 2,..., m (experimental observations). These data are fitted to a function such that $y_i = f(x_i, \alpha, \beta)$, where α and β are two parameters estimated through the chi-square test. Then, the uncertainties associated to each parameter (σ_α and σ_β) are determined by computing the square root of the diagonal elements of the matrix $s^2(W'W)^{-1}$, where

$$s^2 = \frac{\sum (y_i - \hat{y}_i)^2}{m-2} \tag{17}$$

s is the standard deviation and $\hat{y}_i$ the dependent variable estimator. The matrix $(W'W)^{-1}$ is the covariance matrix, and W' is the transposed matrix of W, which elements are

$$w_{ji} = \left(\frac{\partial f(x_i, \theta_j)}{\partial \theta_j} \right) \tag{18}$$

where θ_j are the estimated parameters ($\theta_1 = \alpha$, $\theta_2 = \beta$) and the derivatives are evaluated for the fitted parameters. In our case

$$s^2 = \frac{\sum \left(c_i^{\exp} - c_i^{the} \right)^2}{m-2} \tag{19}$$

being $c_i^{\exp}$ the experimental tritium concentration for observation i and c_i^{the} the theoretical concentration generated for the model considered. If $c_i^{the} = f(t, D, U)$, then the matrix W is

$$W = \left(\begin{array}{cc} \frac{\partial f(t_1, D, U)}{\partial D} & \frac{\partial f(t_1, D, U)}{\partial U} \\ \frac{\partial f(t_2, D, U)}{\partial D} & \frac{\partial f(t_2, D, U)}{\partial U} \\ \cdots & \cdots \\ \frac{\partial f(t_n, D, U)}{\partial D} & \frac{\partial f(t_n, D, U)}{\partial U} \end{array} \right)_{(D_o, U_o)} \tag{20}$$

where D_o and U_o are the optimized longitudinal dispersion coefficient and velocity determined with each model.

DISCUSSION

The optimized longitudinal dispersion coefficient and mean velocity for each field experiment and model are shown in Table 3. As an example, the observed and fitted (numerical model) tritium concentration distribution in Xerta town is also represented (Fig. 5). The optimized longitudinal dispersion coefficient showed large variability as it ranged from 67 ± 20 to 294 ± 36 $m^2\ s^{-1}$. Although the fitted parameters were similar for all models, values obtained with the numerical model were, in general, higher than

those obtained with the analytical and box-type models. This phenomenon has also been observed by other authors and is due to numerical dispersion (Noye, 1987). Although other methods, such as the Lax-Wendroff method, would avoid this problem, this was not considered essential for the purpose of this work. The optimized mean water velocity showed limited variation, as it ranged from 0.575 ± 0.002 to 0.710 ± 0.014 m s^{-1} and the values obtained from the three models at each location were statistically indistinguishable.

In most cases, model fittings were satisfactory as all showed $\chi^2_{0.95} < \chi^2 < \chi^2_{0.05}$. In some locations, the larger χ^2 values observed were due, mainly, to the long tails of the tritium pulses (Fig. 3). Several authors have successfully proposed a dead zone model in which a term is added to the one-dimensional diffusion equation to allow for temporary entrapment of portions of the tracer in the dead zones (Nordin and Troutman, 1980; Yu and Wenzhi, 1989), although this was not the objective of the present work. In other occasions, from Xerta downstream, χ^2 values were too small to be considered valid. At Xerta, some water is deflected and, therefore, flow become lower. As the model is based on a constant flow hypothesis, we concluded that prediction from this point were no longer accurate.

Longitudinal dispersion coefficient

For rivers with similar characteristics to those of the Ebro river (mean width between 120 - 140 m and mean depth between 2.4 - 3.0 m), similar values of the longitudinal dispersion coefficient were observed (Table 4). However, such comparison is only qualitative as, in general, published values of the longitudinal dispersion coefficient do not include uncertainty calculations (Fischer, 1973; Nordin and Troutman, 1980; Mossman *et al.,* 1991; Rutherford, 1994; Graf, 1995).

The longitudinal dispersion coefficient in rivers depends on several factors, as for example river discharge, mean depth, shear velocity, channel width and dead zones. In this study, the variation of the longitudinal dispersion coefficient (Fig. 6) showed three distinct zones, consistent with the observed tritium concentration time distributions (Fig. 3):

1. From Ascó to García (0-10.5 km from the release point): the longitudinal dispersion coefficient at Pas de l'Ase and García (67 ± 20 and 104 ± 17 m^2 s^{-1} respectively) was relatively low. As a consequence, the peaks were relatively sharp and maximum concentration decreased moderately between the two locations.
2. From García to Miravet (10.5-28 km): larger longitudinal dispersion coefficients (256 ± 35 and 257 ± 37 m^2 s^{-1}) caused important diffusion in this section. As a consequence, the tritium concentration peak flattened and broadened considerably at Mora de Ebro in relation to García, in the previous zone. Furthermore, both peaks at Mora de Ebro and Miravet showed long tails which indicated the presence of dead zones in this section. This is due to the increase of width channel and the decrease of river depth, including island deposition.
3. From Miravet to Tortosa (28-63.5 km): in this zone the maximum tritium concentration decreased only slightly and the peak shape was more symmetrical and almost unchanged from Benifallet. This was in agreement with lower longitudinal dispersion coefficients (ranging from 147 - 79 m^2 s^{-1}) which caused little effect on the tracer distribution shape. Downstream Xerta, tracer transport became more complex because a channel diverts some water at this location and downstream Tortosa estuarine effects start to become apparent.

To study diffusion it is necessary to take into account channel geometry, slope, dead zones, meanders, sinuosity, ... In consequence, the most accurate method to determine

the longitudinal dispersion coefficient in rivers is experimentally using a tracer. In Eq. (1) D is assumed to be constant, which reduces complexity of the solutions and, in this study, permitted the comparison of the various approaches to solving the proposed problem. However, this was not the case, as the coefficient is largely dependent on river flow and morphology. A more complete study on the hydrodynamics of the river should consider its variability with this, although this was not the objective of the present work.

Mean water velocity

Usually, water velocity is determined as a function of river morphology using the Manning equation (Chow *et al.,* 1988)

$$U = \frac{R^{2/3} S^{1/2}}{n} \tag{21}$$

where R is the hydraulic radius, that is, the ratio of the cross-sectional area to the wetted perimeter, S is the slope and n is the Manning roughness coefficient. However, needed field measurements and/or theoretical determination of these parameters are beyond the objectives of this work.

The functional relationship between mean water velocity and river discharge can be described with a power function (Knighton, 1984; Morisawa, 1985). Although in this field experiment the flow rate was constant, a power relationship was derived from experiments carried out during 1991 in the same area (Sanchez-Cabeza *et al.*, 1992) and used to predict velocity for the experimental design. However, this velocity was overestimated because the power function does not take into account the changes in river morphology. The overestimation was more evident far away from the release point, as it is observed in Tortosa and Amposta (Fig. 3 and Fig. 4).

At 100 km upstream from the river mouth, before the Ascó nuclear power plant, the river meets the mountains of the Catalan Chain. In this area, river slope is important,

mean depth water and channel width are *circa* 4.2 m and 140 m respectively, so mean water velocity is relatively high, as observed in Pas de l'Ase (Fig. 7). Then, the river enters the Mora Depression and river velocity is reduced because the slope decreases and the transversal section of the river (mean water depth and channel width are 2.5 m and 180 m, respectively) becomes flatter, that is, the hydraulic radius decreases. At Miravet and Benifallet, both slope and hydraulic radius are still relatively large and mean water velocity increases considerably. The Xerta weir is located at 60 km from the river mouth and, consequently, an important velocity reduction is observed because of the low slope in this zone. Similarly, the mean water velocity in Tortosa is also low due to the lower slope of this final section.

Finally, river velocity in Amposta deserves special mention because it is not only affected by river morphology but also by the interaction with marine waters, which cause an important reduction of mean water velocity. This fact, together with the extension of this study to a wide range of river discharges and the determination of key morphological parameters, merit further research in the future.

CONCLUSIONS

Tritium routinely released as low-activity liquid radioactive waste by the Ascó nuclear power plant (Tarragona, Spain), was used as a radiotracer to determine the longitudinal dispersion coefficient and the mean velocity of the Ebro river waters (northeastern Spain). This was made possible by the use of a rapid and sensitive technique for the detection of low tritium concentrations in river waters.

The one-dimensional advection-diffusion equation was solved for the case of a non instantaneous tracer release. The longitudinal dispersion coefficient and the velocity of Ebro river waters were determined through the use of three different models: analytical,

box-type and numerical. The models reliability was confirmed by the homogeneity of the results.

For the river discharge attained during the field experiment, namely 220 m^3 s^{-1}, longitudinal dispersion coefficient ranged from 67 ± 20 to 294 ± 36 m^2 s^{-1} and mean velocities ranged from 0.575 ± 0.002 m s^{-1} to 0.710 ± 0.014 m s^{-1} depending on the sampling location. The observed longitudinal dispersion coefficients showed the presence of three distinct zones in the lower course of the Ebro river and confirmed that dispersion depends largely on river morphology. This is also the case for mean water velocity as river slope, hydraulic radius and natural or artificial accidents can qualitatively explain the observed differences.

The results of this work can be used to predict the movement and dispersion of a soluble substance in the Ebro river downstream the nuclear power plant and may permit to design adequate surveillance programs and emergency actions in the case of the accidental release of a soluble radioactive or non-radioactive substance.

Acknowledgements

Financial support received from *Junta de Sanejament de la Generalitat de Catalunya* is gratefully acknowledged. Also, we wish to express our gratitude to *Asociación Nuclear Ascó* for its collaboration with this study and for making available important information for its scientific development, and to *Confederación Hidrográfica del Ebro*, *Embalse de Ribaroja* and *Embalse de Flix* for their collaboration in maintaining constant flow rate during the sampling campaign. Thanks are due to colleagues in our Department and to others for collaboration in the sampling campaign.

REFERENCES

Abril, J.M. and García León, M. (1992) A marine dispersion model for radionuclides and its calibration from non-radiological information, *J. Environ. Radioactivity* **16**, 127-146.

APHA-AWWA-WEF (1992), *Standard Methods for the Examination of Water and Wastewater; American Public Health Association,* 18th ed., Washington.

Bertin, C. and Bourg, A.C.M. (1994) Radon-222 and chloride as natural tracers of the infiltration of river water into an alluvial aquifer in which there is significant river/groundwater mixing, *Environ. Sci. Technol.* **28**, 794-798.

Clark, J.F., Schlosser, P., Stute, M. and Simpson, H.J. (1996) SF6 – 3He tracer release experiment: a new method of determining longitudinal dispersion coefficients in large rivers, *Environ. Sci. Technol.* **30**, 1527-1532.

Cuadras, C.M. (1991) *Problemas de probabilidad y estadística,* Promociones y Publicaciones Universitarias S.A., Barcelona, 452 pp (in Spanish).

Chow, V.T., Maidment, D.R. and Mays, L.W. (1988) *Applied Hydrology*, McGraw-Hill Book Company, New York, 572 pp.

Day, T.J. (1975) Longitudinal dispersion in natural channels, *Water Resour. Res.* **11**, 909-918.

Day, T.J. (1977) Observed mixing lengths in mountain streams, *J. Hydrology* **35**, 125-136.

Fischer, H.B. (1973) Longitudinal dispersion and turbulent mixing in open-channel flow, *Ann. Rev. Fluid Mech.* **5**, 59-78.

Forés, E., Menéndez, M. and Ibáñez, C. (1992) The Ebro River Delta, in: *Proc. XXV SIL Congress* (Edited by Catalán, J. and Pretus, J.Ll.), Barcelona.

Graf, J.B. (1995) Measured and predicted velocity and longitudinal dispersion at steady and unsteady flow, Colorado River, Glen Canyon Dam to Lake Mead, *Water Resour. Bull.* **31**, 265-281.

Guillén, J. and Palanques, A. (1992) Sediment dynamics and hydrodynamics in the lower course of a river highly regulated by dams: the Ebro River, *Sedimentology* **39**, 567-579.

Guizerix J. and Florkowski, T. (1983) Streamflow measurements, in: *Guidebook on Nuclear Techniques in Hydrology*, IAEA, Vienna, 65-79.

Hancock, G.J. and Murray, A.S. (1996) Source and distribution of dissolved radium in the Bega River estuary, Southeastern Australia, *Earth Planet. Sci. Lett.* **138**, 145-155.

IAEA (1985) *Hydrological dispersion of radioactive material in relation to nuclear power plant siting*, IAEA, Vienna, 116 pp.

Ibáñez, C., Prat, N. and Cancio, A. (1996) Changes in the hydrology and sediment transport produced by large dams on the lower Ebro river and its estuary, *Regul. Riv.* **12**, 51-62, 1996.

Keith, L.H., Crummett, W., Deegan, J., Libby, R.A., Taylor, J.K., Wentler, G. and ACS Committee on environmental improvement (1983) Principles of environmental analysis, *Anal. Chem.* **55**, 2210-2218.

Knighton, D. (1985) *Fluvial forms and processes*, Edward Arnold, London, 218 pp.

Kopman, D.B. and Voss, C.I. (1987) Behavior of sensitivities in the one-dimensional advection-dispersion equation: implications for parameter estimation and sampling design, *Water Resour. Res.* **23**, 253-272.

Morisawa, M. (1985) *Rivers*, Longman Group Limited, New York.

Mossman, D.J., Holly, F.M. and Schnoor, J.L. (1991) Field observations of longitudinal dispersion in a run-of-the-river impoundment, *Wat. Res.* **11**, 1405-1415.

Nordin, C.F. and Troutman, B.M. (1980) Longitudinal dispersion in rivers: the persistence of skewness in observed data, *Water Resour. Res.* **16**, 123-128.

Noye, J. (1987) Finite difference methods for solving one-dimensional transport equation, in: *Numerical modelling: applications to marine systems* (Edited by Noye, J.), Elsevier Science Publishers B.V., North-Holland, 231-256.

Palanques, A., Plana, F. and Maldonado, A. (1990) Recent influence of man on the Ebro margin sedimentation system, northwestern Mediterranean Sea, *Mar. Geol.* **95**, 247-263.

Prandle, D. (1984) A modelling study of the mixing of ^{137}Cs in the seas of the european continental shelf, *Phil. Trans. R. Soc. Lond.* **A 310**, 407-436.

Pujol, Ll. (1996) *Radiactividad del agua superficial y los sedimentos en la cuenca del Ebro. Utilización del tritio como radiotrazador en el tramo catalán*, Ph. D. Thesis, Universitat Autònoma de Barcelona, 182 pp (in Spanish).

Pujol, Ll. and Sanchez-Cabeza (1997) Radiactividad del agua superficial y los sedimentos en la cuenca del Ebro. Utilización del tritio como radiotrazador en el tramo catalán. *Radioprotección* **15**, 95-103 (in Spanish).

Rawlings, J.O. (1988) *Applied Regression Analysis, A Research Tool*, Wadsworth, Inc., California, 553 pp.

Rutherford, J.C. (1994) *River Mixing*, John Willey and Sons, New York, 347 pp.

Sanchez-Cabeza, J.A., Pujol, Ll., Molero, J., Merino, J., León, L., Vidal-Quadras, A., Schell, W.R., Trilla, J. and Mitchell, P.I. (1992) Estudio preliminar sobre el transporte de especies químicas solubles en el río Ebro utilizando el tritio como

trazador, in: *Actas de la XVIII Reunión Anual de la Sociedad Nuclear Española,* Senda Editorial, S.A., Madrid, 25-27 (in Spanish).

Sanchez-Cabeza, J.A., Pujol, Ll., Merino, J., León, L., Vidal-Quadras, A., Schell, W.R. and Mitchell, P.I. (1993) Optimization and calibration of a low background liquid scintillation counter for the simultaneous determination of alpha and beta emmitters in aqueous samples, in: *Liquid Sicntillation Spectrometry 1992* (Edited by Noakes, J.E., Polach, H.A. and Schönhoffer, F.), Radiocarbon, 43-50.

Sanchez-Cabeza, J.A., Molero, J., Merino, J., Pujol, Ll. and Mitchell, P.I. (1995) ^{137}Cs as a tracer of the Catalan current, *Oceanologica Acta* **18**, 221-226.

Scott, E.M. (1994) Simple environmental models for radioactive dispersal in the marine environment, in: *Low-level measurements of radioactivity in the environment. Techniques and applications* (Edited by García-León, M. and García-Tenorio, R.), World Scientific, Singapore, 447-460.

Van Genuchten, M.T. and Alves, W.J. (1982) *Analytical Solutions of the One-Dimensional Convective-Dispersive Solute transport Equation*, TYechnical Bulletin No. 1661, United States Department of Agriculture, Washington, 149 pp.

Yotsukura, N. and Sayre, W.W. (1976) Transverse mixing in natural channels, *Water Resour. Res.* **12**, 695-704.

Yu, Y.S. and Wenzhi, L. (1989) Longitudinal dispersion in rivers: a dead-zone model solution, *Water Resourc. Bull.* **25**, 319-325.

Table 1. Characteristics of the tritium release from Ascó nuclear power plant (Asociación Nuclear Ascó, personal communication).

Date	May 19, 1992
Release start	9:00
Release duration (min)	105
Volume released (m^3)	21.7
Tritium activity (GBq m^{-3})	3.5261
River discharge (m^3s^{-1})	220
Mixing activity (Bq l^{-1})	55.2

Table 2. Sampling information.

Sampling location†	Date	Latitude (N)	Longitude (E)	Distance‡ (km)	Sampling period
Ascó	19/5/92	41º 11' 05"	0º 34' 20"	0.5	09:00 - 13:00
Pas de l'Ase	19/5/92	41º 09' 55"	0º 36' 45"	6.5	10:30 - 15:30
García	19/5/92	41º 08' 15"	0º 38' 55"	11.0	12:00 - 17:15
Mora de Ebro	19/5/92	41º 05' 55"	0º 38' 30"	16.0	14:00 - 22:00
Miravet	19-20/5/92	41º 02' 00"	0º 36' 35"	28.0	16:00 - 01:30
Benifallet	19-20/5/92	40º 58' 45"	0º 31' 15"	39.0	19:30 - 06:30
Xerta	19-20/5/92	40º 55' 25"	0º 29' 30"	47.5	23:30 - 11:30
Tortosa	20/5/92	40º 48' 50"	0º 31' 15"	63.5	03:30 - 16:30
Amposta	20/5/92	40º 42' 45"	0º 35' 10"	78.0	08:00 - 23:00

†See Figure 2.
‡From Ascó nuclear power plant.

Table 3. Summary of the optimized parameters determined with the different models.

Location	Model	U_o (m s^{-1})	D_o (m^2 s^{-1})	χ^2	$\chi^2_{0.95}$	$\chi^2_{0.05}$
Pas de l'Ase	Analytical	0.689 ± 0.013	67 ± 20	12.3	3.94	18.3
(May 19, 1992)	Box-type	0.710 ± 0.014	70 ± 21	12.2	3.94	18.3
	Numerical	0.689 ± 0.013	105 ± 20	12.2	3.94	18.3
García	Analytical	0.645 ± 0.009	104 ± 17	15.0	6.57	23.7
(May 19, 1992)	Box-type	0.663 ± 0.009	106 ± 17	15.2	6.57	23.7
	Numerical	0.645 ± 0.009	140 ± 17	14.8	6.57	23.7
Mora de Ebro	Analytical	0.580 ± 0.011	256 ± 35	21.0	10.1	30.1
(May 19, 1992)	Box-type	0.611 ± 0.011	264 ± 35	20.5	10.1	30.1
	Numerical	0.579 ± 0.011	289 ± 35	20.7	10.1	30.1
Miravet	Analytical	0.664 ± 0.009	257 ± 37	32.9	15.4	38.9
(May 19-20, 1992)	Box-type	0.682 ± 0.009	261 ± 36	31.9	15.4	38.9
	Numerical	0.664 ± 0.009	294 ± 36	32.4	15.4	38.9
Benifallet	Analytical	0.652 ± 0.005	147 ± 18	25.4	15.4	38.9
(May 19-20, 1992)	Box-type	0.656 ± 0.005	149 ± 18	23.7	15.4	38.9
	Numerical	0.648 ± 0.005	182 ± 17	24.9	15.4	38.9
Xerta	Analytical	0.577 ± 0.002	90 ± 6	6.9	12.3	33.9
(May 19-20, 1992)	Box-type	0.579 ± 0.002	90 ± 6	6.1	12.3	33.9
	Numerical	0.575 ± 0.002	121 ± 6	6.7	12.3	33.9
Tortosa	Analytical	0.585 ± 0.001	79 ± 2	0.6	6.57	23.7
(May 20, 1992)	Box-type	0.587 ± 0.001	79 ± 2	0.6	6.57	23.7
	Numerical	0.584 ± 0.001	110 ± 2	0.6	6.57	23.7

Uncertainties correspond to ± 1σ.

Table 4. Reported longitudinal dispersion coefficients for rivers with similar characteristics to those of the Ebro river (including data from Rutherford, 1994).

River	Mean depth (m)	Mean width (m)	Mean velocity (m s^{-1})	Discharge (m^3 s^{-1})	Dispersion coefficient (m^2 s^{-1})
Missouri	2.70	200	1.55	837	1500
	2.33	183	0.89	380	465
Sabine	2.04	104	0.58	119	316
	4.75	128	0.64	389	670
Yadkin	2.33	70	0.43	71	111
	3.85	72	0.76	213	260
Waikato	2.60	85	0.69	153	52
	2.00	120	0.64	153	67
Ebro	*2.4 - 3.0*	*120 - 140*	*0.56 - 1.28*	*178 - 915*	*41 - 392*

Figure 1. Ebro river basin and physiographical elements.

Figure 2. Map of the studied section of the Ebro river showing sampling locations.

Figure 3. Tritium concentration as a function of time after a low-activity liquid radioactive waste release from Ascó nuclear power plant, May 19-20, 1992.

Figure 4. Tritium concentration at Amposta, May 20, 1992.

Figure 5. Tritium concentration at Xerta May 19-20, 1992. The solid line shows the optimum numerical model fit (explicit finite differences).

Figure 6. Longitudinal dispersion coefficient from the release point (analytical model). The dotted line corresponds to the mean value for each zone.

Figure 7. Mean water velocity as a from the release point (analytical model).

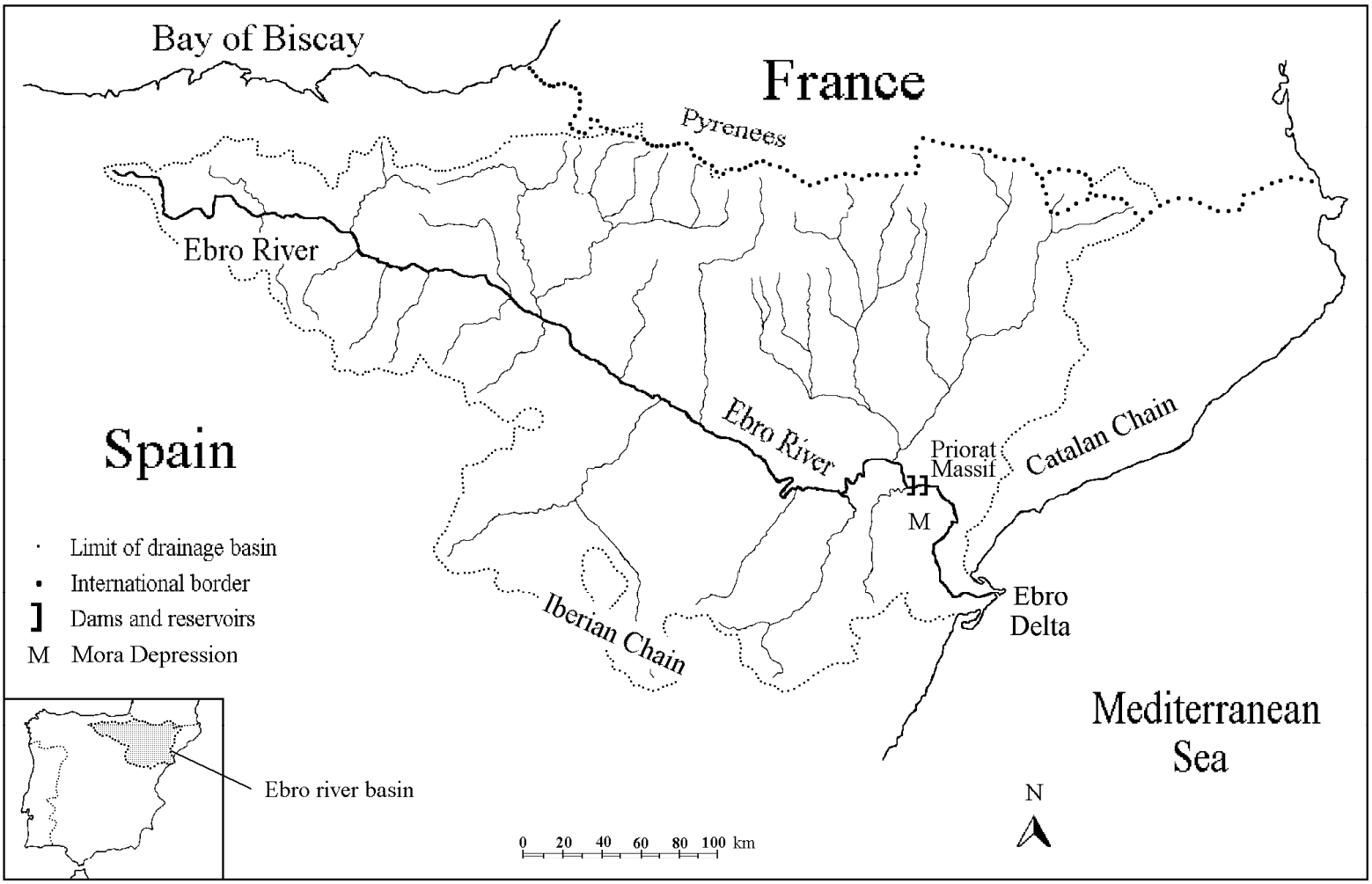
Bay of Biscay
France
Pyrenees
Ebro River
Spain
Ebro River
Priorat Massif
Catalan Chain
M
Iberian Chain
Ebro Delta
Mediterranean Sea
· Limit of drainage basin
• International border
] Dams and reservoirs
M Mora Depression
Ebro river basin
0 20 40 60 80 100 km
N

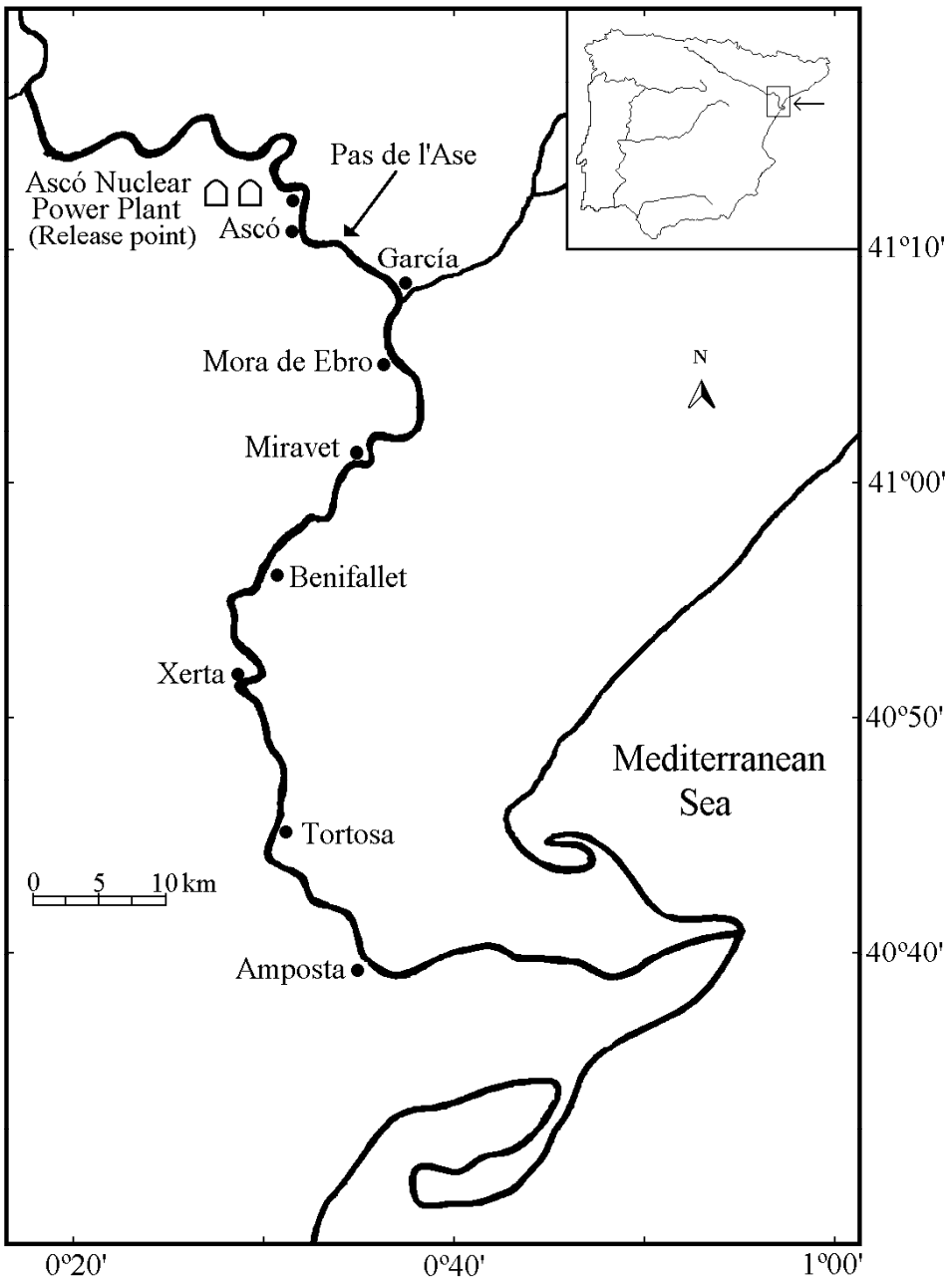
Pas de l'Ase
Ascó Nuclear
Power Plant
(Release point)
Ascó
García
Mora de Ebro
Miravet
Benifallet
Xerta
Tortosa
Amposta
Mediterranean
Sea
N
0 5 10 km
41°10'
41°00'
40°50'
40°40'
0°20'
0°40'
1°00'

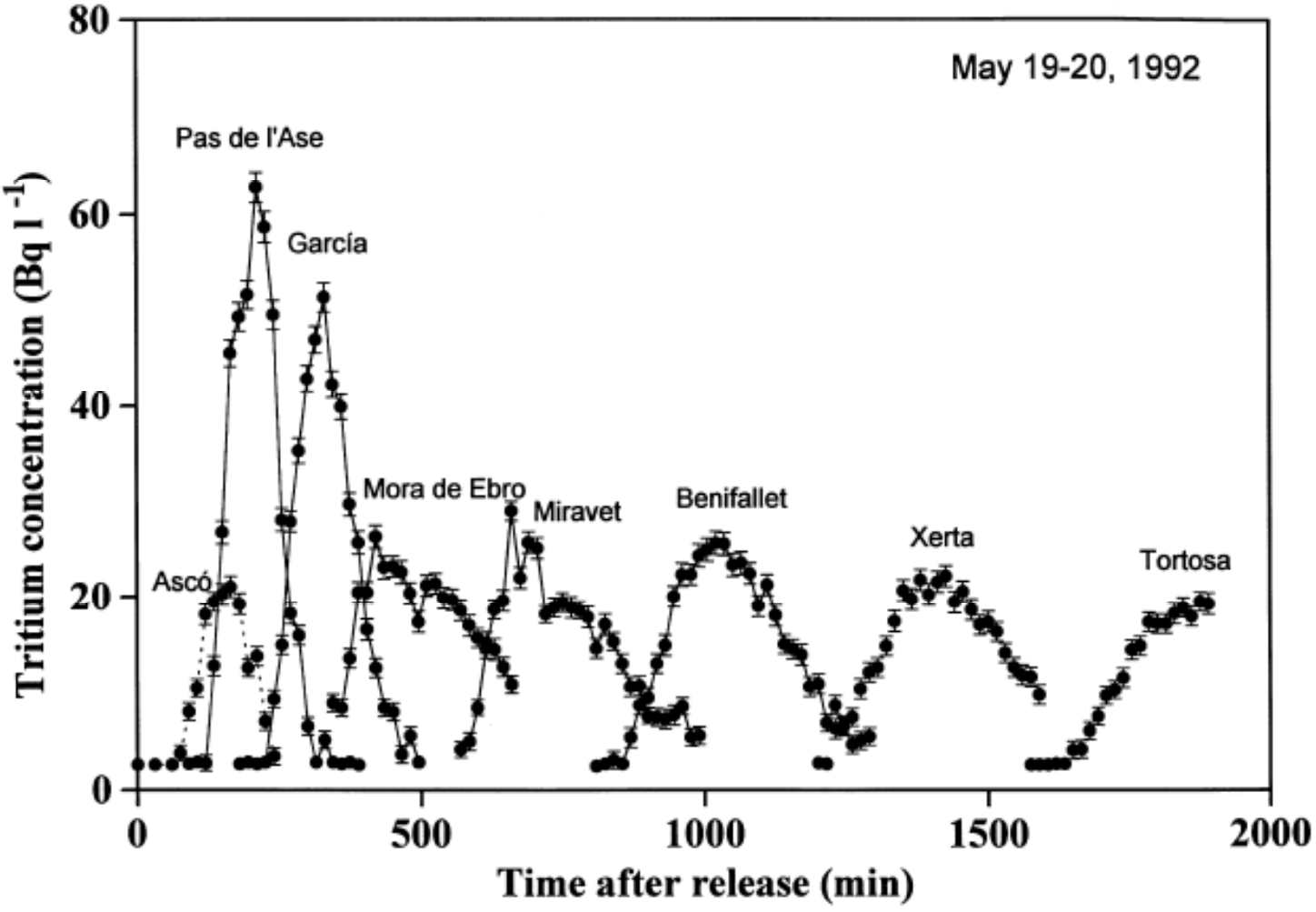
May 19-20, 1992
Pas de l'Ase
García
Ascó
Mora de Ebro
Miravet
Benifallet
Xerta
Tortosa
Tritium concentration (Bq l-1)
Time after release (min)
0
20
40
60
80
0
500
1000
1500
2000

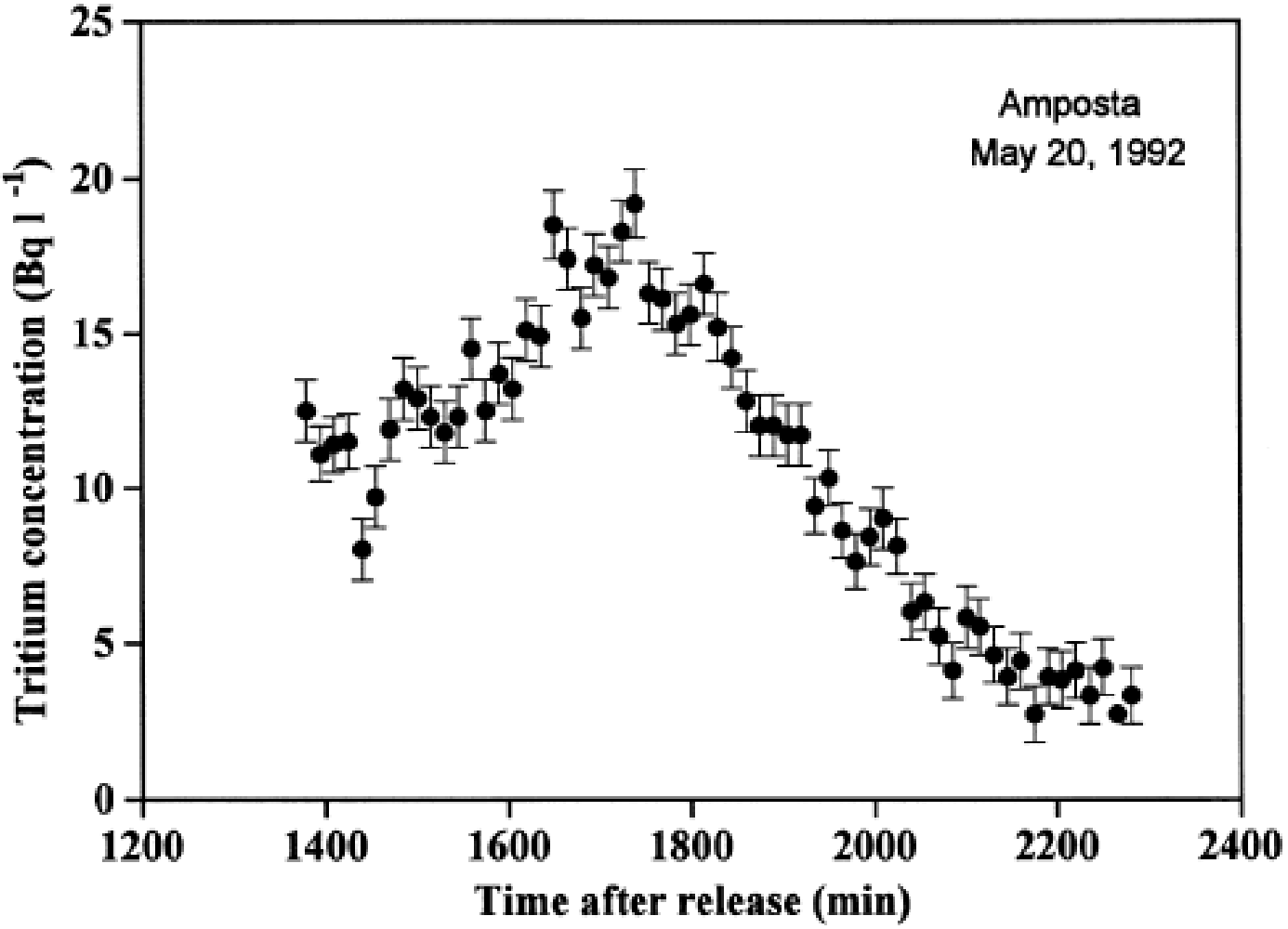
Amposta
May 20, 1992
Tritium concentration (Bq l-1)
Time after release (min)
0
5
10
15
20
25
1200
1400
1600
1800
2000
2200
2400

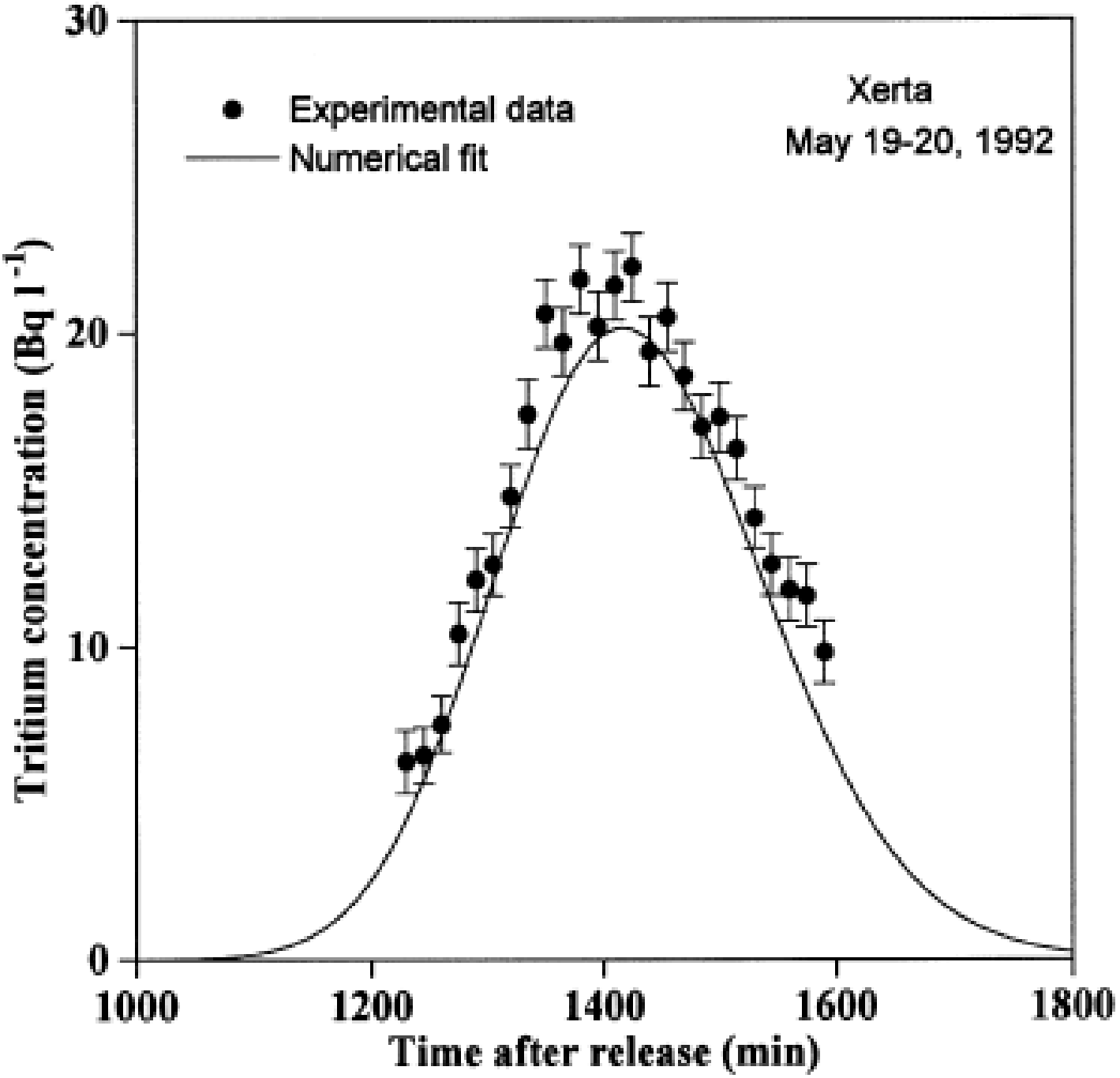
Experimental data
Numerical fit
Xerta
May 19-20, 1992
Tritium concentration (Bq l-1)
Time after release (min)
0
10
20
30
1000
1200
1400
1600
1800

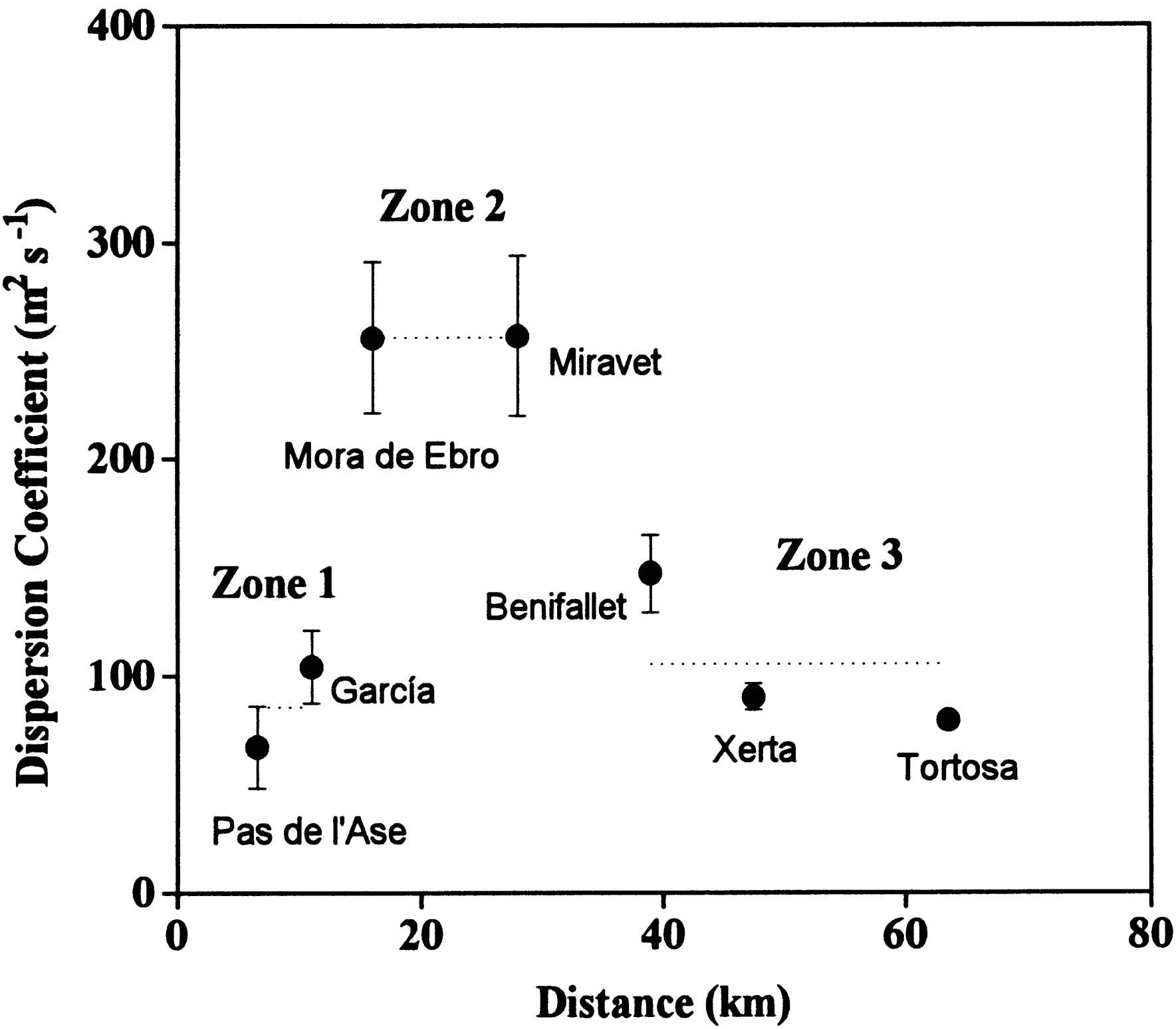
Zone 2
Miravet
Mora de Ebro
Zone 1
Zone 3
Benifallet
García
Xerta
Tortosa
Pas de l'Ase
Dispersion Coefficient (m2 s-1)
Distance (km)
0
100
200
300
400
0
20
40
60
80

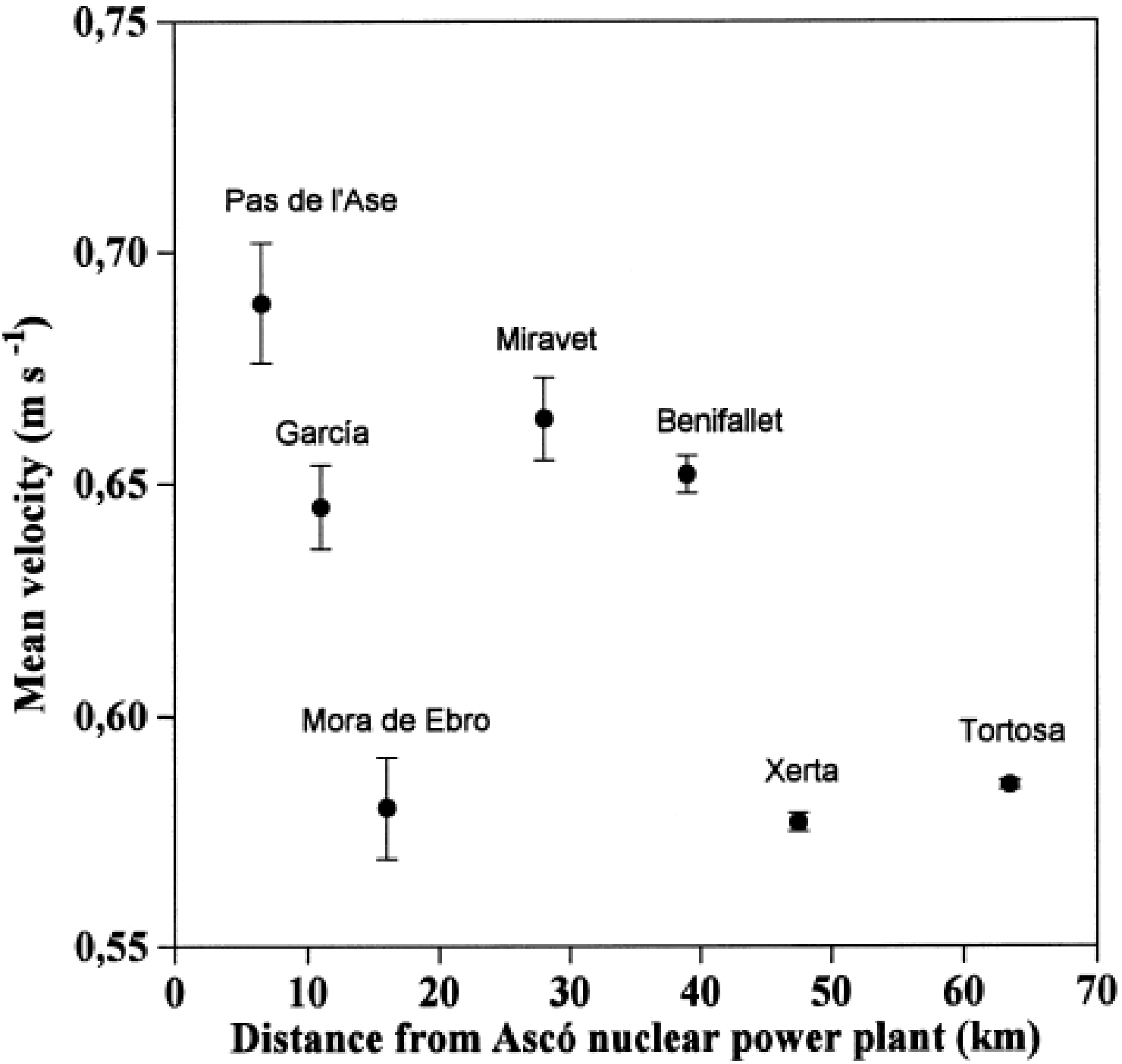
0,75
0,70
0,65
0,60
0,55
Mean velocity (m s -1)
Pas de l'Ase
García
Miravet
Benifallet
Mora de Ebro
Xerta
Tortosa
0
10
20
30
40
50
60
70
Distance from Ascó nuclear power plant (km)